Journal of Materials Science Research and Reviews

8(2): 1-12, 2021; Article no.JMSRR.69830

Numerical Simulation and Microstructural Correlation of Duplex Stainless Steel Solidification by Spray-Forming Process

Moises Meza Pariona[1*] and Luiz Gustavo Kobilacz[1]

[1]State University of Ponta Grossa, Department of Materials Engineering, Ponta Grossa-PR, Brazil.

Authors' contributions

This work was carried out in collaboration between both authors. The author LGK drew the geometries. Author MMP did the simulation and wrote the article. Both authors read and approved the final manuscript.

Article Information

Editor(s):
(1) Dr. Chong Leong, Gan, Micron Memory Taiwan Co. Ltd, Taiwan.
Reviewers:
(1) Wang Lina, Hainan Normal University, China.
(2) Guy Francis Mongelli, Case Western Reserve University, USA.
Complete Peer review History: http://www.sdiarticle4.com/review-history/69830

Original Research Article

Received 10 April 2021
Accepted 16 June 2021
Published 24 June 2021

ABSTRACT

Duplex stainless steel are designed to provide better corrosion resistance, particularly chloride stress corrosion and chloride pitting corrosion, and higher strength than standard austenitic stainless steels. In Spray Forming processing, the gas atomizes a liquid metal stream and is generated a number of high velocity gas jets and is broken up into fine drops which solidify in flight and finally is captured the atomized metal spray of alloy onto a moving substrate into near net shape solid. In this research was be presented a thermal model for modeling the heat flow distribution during solidification process and the heat transfer analysis using finite element modeling was carried out, to study of solidification of droplet deposition in spray-forming process and its correlation with microstructure. For this purpose, was assumed a Gaussian distribution of droplet mass flux about the spray cone axis, boundary conditions non-linear of heat transfer coefficient and thermophysical properties dependent with temperature, the spray forming process parameters, such as, fluid pressure, geometrical parameter of the nozzle's dimensionless characteristic, temperature of the saturation, workpiece height, thickness of the bottom's sprayer were considerate too. As result were presented a solidification process analysis, study of thermal gradient, cooling curves analysis and correlation between numerical simulation and microstructural

**Corresponding author: Email: mmpariona@uepg.br;*

result. The microstructure analysis was used to establish the correlation with numerical simulation for has better performance of prevision. Duplex stainless steels are applied in various strategic areas, which are finding greater application in the chemical, oil and gas industries, petrochemical process plants, pollution control equipment, etc. Numerical simulation is a powerful tool to study the spray-forming process, whose parameters that involve this process can save runtime experimental and cost of equipment, besides, predict the result.

Keywords: Spray-forming; solidification; heat flow; FEM; microstructure; SEM.

NOMENCLATURE

c_p specific heat capacity, J/(kg.K)
F nozzle's orifice area, m^2
$g(x, y)$ dispersion function, $m^3/(m^2.s)$
$gmax(0)$ maximum dispersion (surface center), $m^3/m^2.s$
h_g the heat transfer coefficient at the upper surface of the work piece, $W/(m^2.K)$
h_a the convection coefficient exposed to atmospheric air, $W/(m^2.K)$
h depth of the sprayer slit, m
H height of the nozzle up to workpiece (0.6 m)
k thermal conductivity, W/(m.K)
p fluid pressure, Pa
R inner radius of the sprayer channel, m
q heat flux, W/m^2
ζ, geometrical parameter of the nozzle's dimensionless characteristic (ζ =h-δ/2R)
ρ density, kg/m3
σ variance
ψ fluid statistical parameter, $kg/(m^2.s)$
T_w temperature of the wall
T_a temperature of the ambience (300 K)
T_{sat} temperature of the saturation (1609 K)
T_i initial temperature (1650 K)
wh workpiece height (0.24 m)
φ opening angle of the sprayer (60 deg)
δ thickness of the bottom's sprayer, m
ε surface emissivity (0.22)

1. INTRODUCTION

Duplex stainless steels (DSSs) represent a class of stainless steels with dual microstructure consisting of approximately equal proportions of ferrite and austenite phases. This balanced microstructure offers a favorable combination of mechanical strength and corrosion resistance. The volume fractions of ferrite and austenite in welded DSSs depends upon the thermal history. Owing to their superior mechanical properties and corrosion characteristics, DSSs have been employed as structural materials in various industrial sectors, such as offshore construction, chemical, petrochemical, pulp and paper, power generation, desalination, and oil and gas. Recently, in view of increasing applications of DSSs, it is important to have a better understanding of the issues associated with welding of DSSs. this study was confirmed by authors Daha et al. [1] and del Coz Díaza et al. [2]. However, this last author reported that the thermal expansion in the duplex grades is intermediate to that of carbon steel and the austenitic stainless steels. The thermal conductivity in duplex stainless steels is also intermediate that of carbon steels and the austenitic stainless steels. Duplex stainless steels, with higher thermal conductivity and lower coefficient of thermal expansion, do not create the same high intensity of local thermal stresses in the welds of austenitic stainless steels.

1.1 Description of the Problem

Since its invention in the 1970s, spray forming has developed steadily to become a niche casting technology for highly alloyed metallic alloys, including hypereutectic Al-Si alloys, high-speed steels, Ni superalloys, etc. It has become a standard industrial practice to use a melt-atomization system for the spray forming of Al, Cu, and steel preforms in a large-volume production, this was reported by Zhang et al. [3]. Spray forming is an integrated melt atomization and droplet deposition process that involved transport phenomena. The basic physics involved are: (1) the fragmentation of a continuous liquid stream into discrete droplets, (2) multi-phase flow of the gas-droplet spray and non-linear heat transfer, (3) droplet deposition, splashing and redeposition at a deposition surface, and (4) pre-form solidification and microstructural evolution, supported by Mi and Grant [4]. In the spray forming process, the heat transferred from depositing droplets to a growing preform in deposition, and the subsequent heat flow/solidification inside the preform, which govern the microstructural evolution of the preform [4].

Kumar et al. [5] discussed the advantages of the spray-forming technique, spray forming process is a material processing technology in which molten metal is transformed into near net shape solid of refined microstructure without any intermediate processing steps. These authors add, the process is characterized by capturing a spray of gas atomized metal or alloy droplets onto a moving substrate. In this process solidification takes place in two stages, where solidification begins at higher rate when metal droplet is in air and completes at slower rate when the same is on substrate. These authors also point out, the high cooling rate and fast solidification of atomized molten particles leads to the formation of fine grained and more homogeneous microstructure without macro-segregation, as compared to conventionally made products. Spray forming process can be used to manufacture alloy compositions which are problematic when produced using conventional process, which was highlighted by Mi and Grant [4].

During droplet deposition process that involved transport phenomena that can happen several cases, among them, a fraction of the arriving mass is retained on the surface at the point of impact, and therefore contributed to the growth of the surface of that point towards the incident mass and the remainder of the arriving mass is assumed to splash or rebound away from the surface, however, for solid particles, this scattering might occur by rebounding, whereas splashing was found to be important for substantially large liquid droplets, can also occur, the scattered mass either redeposited elsewhere on the surface, contributing to the growth of the surface at that point or was lost from the system as overspray, this fact has been confirmed by Mi and Grant [4] investigated that the ratio of the retained mass over the total mass arriving at a given point is commonly defined as the ‘‘sticking efficiency” SE, which depends on: (1) the geometrical and thermal conditions of the deposition surface, (2) the kinetic energy and thermal conditions of the impacting droplets, and (3) the interactions between the deposition surface and the impacting droplets. Nevertheless, Mia et al. [6] affirmed that spray forming is an inherent Multiphysics process consisting of multi-length (micrometers to meters) and multi-timescale (microseconds to minutes) transport phenomena

2. STATE OF THE ART

2.1 Modeling the Deposition Generated by Atomizer of Spray-forming System

However, the challenging aspects which hinder the successful adoption of FEM in the spray-forming process sector applied in manufacturing industry should be solved first. One of the greatest challenges is the identification of the correct set of numerical simulation input parameters. Between them involves, the thermophysical properties of the material and the application of boundary conditions, where the physical parameters are not constants.

The thermophysical properties of the 21Cr-6Ni-9Mn alloy as a function of temperature was considered in this work, the properties of this alloy were reported by Comsol [7] and Mi and Grant [4], For this purpose, a workpiece geometry in 3D was built, this was a replica of the experimental result presented by the authors Zepon et al. [8] and Caoa et al. [9]. Finite element analysis in this investigation using a full three-dimensional thermal finite element formulation of the heat transfer conduction during solidification of droplet deposition was performed and it was simulated by sequentially coupled formulation, considering the geometric model, materials properties, workpiece mesh, initial condition and boundary condition applied on the workpiece. The solution process was performed in transient mode and thermal finite element formulation was implemented in Comsol Multiphysics [7]. Finally, a correlation of the numerical simulation result with the microstructure was performed.

The heat transfer in cross-sectional shapes was simulated using the primary deposition, plus redeposition model of droplets, however, the scattered mass that was lost from the system as overspray and it wasn´t considered in this study. In Fig. 1 is presented a 3D geometrical sketch of the spray-forming process, where the metal-droplet spray flow was considerate with a Gaussian distribution behavior.

In the next, at the workpiece a mesh with tetragonal elements was made. In Fig. 2 is shown the geometry model and the workpiece mesh.

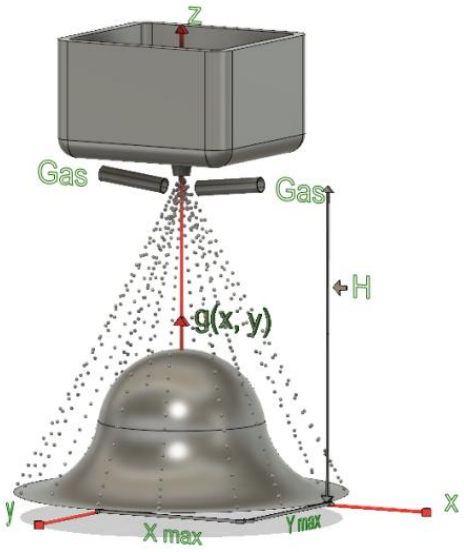

Fig. 1. A 3D geometrical sketch of the spray-forming process, showing the heat transfer of the metal-droplet spray flow, considerate with a Gaussian distribution behavior

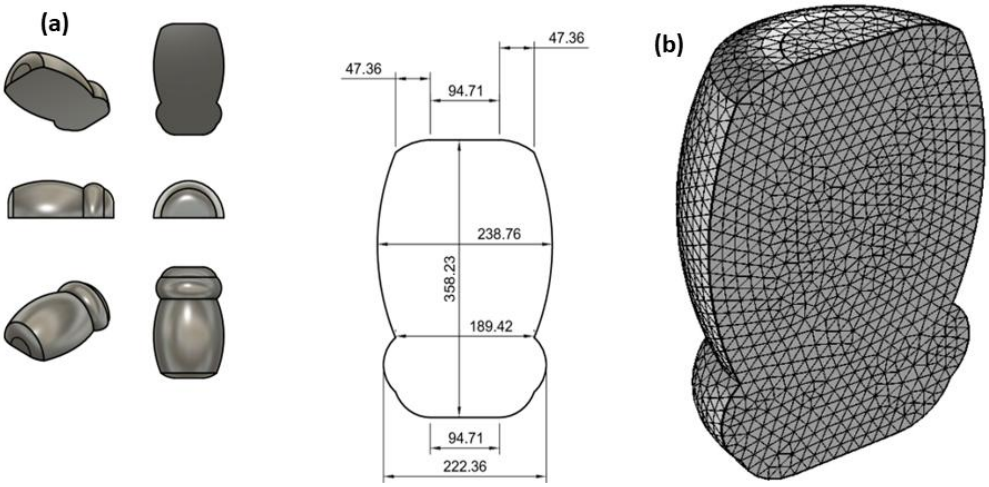

Fig. 2. (a) geometry model in 3D and (b) finite element model

2.2 Governing Equations for Boundary Conditions

The equations that govern the thermal field will be presented in this section section. In application of boundary conditions in thermal finite element formulation, the physical parameters are not constants or non-linear heat transfer occurs. The following equation was proposed by Mzad and Khelif [10].

$$g(x,y) = g_{max}(0).\exp\left[0.5\left(\frac{x^2}{x^2_{max}.\sigma^2_x} + \frac{y^2}{y^2_{max}.\sigma^2_y}\right)\right. \quad (1)$$

Equation (1) represents normal dispersion of the droplet jet over the surface. Were the dispersion $g_{max}(x,y)$ is along of the axes *y* and *x* and in function of Gmax(0), x_{max} and y_{max} (representation of these parameters is shown in Fig. 1), since these parameters are depending on the nozzle's geometrical characteristics, as well as, of the parameters, such as ΔP (the pressure of the spray), H high of the spray nozzle in relation to the wet workpiece surface and mass density (ρ) of the liquid metal.

Through of statistical methods and with a basis experimental was established by Mzad and Khelif [10], the following equation.

$$g_{max(0)=2.10239.\Psi^{1.206}.\xi^{-0.702}} \quad (2)$$

The x_{max} and y_{max} depend on the height H, tgφ/2 and F section area of the sprayer aperture, thus, so that x_{max} and y_{max} are also proportional to the number K2 = H.tgφ/2 and F. Then, through the mean value of all the experimental data, the following correlations were established by Tebbal and Mzad [11], and Mzad and Khelif [10], the subsequent equations.

$$x_{max} = 24120.K_2^{-0.468} \quad (3)$$

$$y_{max} = 21.27.K_2^{-0.062} \quad (4)$$

The fluid dispersion field on the surface is described by the equation and it has an elliptical form.

$$\left(\frac{x}{x_{max}}\right)^2 + \left(\frac{y}{y_{max}}\right)^2 = 1 \quad (5)$$

Ψ is fluid statistical parameter, kg/(m^2 s) and ζ is a specific dimensionless geometrical characteristic of the nozzle used. In our case, ζ= 0.225 and the nozzle's orifice section area *F* = 180 mm^2 with an opening angle of 60° and p=1x10^5 Pa.

Heat transfer rate is proportional to the dispersion *g*(*x*, *y*) and impinging fluid pressure *p*, it was shown that non-linear heat transfer in flow of the metal-droplet spray can be estimated using the correlation, which it was proposed by Mzad and Khelif [10].

$$q=4.6x10^6.p^{0.1}.g^{0.4} \quad (6)$$

The equation governing the three-dimensional transient heat conduction problem is as follows:

The convection boundary condition can be expressed as, [10]

$$\begin{cases} \rho.c_p.\frac{\partial T}{\partial t} + \nabla.(-k\nabla T) = 0, \\ T(t=0) = 1650\ K \end{cases} \quad (7)$$

Boundary conditions are set under Newton-Riemann assumption, it was considered on the workpiece surface to be solidified in the lower part and on the sides, such as, [10]:

$$-n.(-k\nabla T) = h_a.(T_w - T_a) \quad (8)$$

As well as, in the upper part of the work piece was considered the influence of the fluid dispersion field, which is presented by Gaussian distribution of droplet mass flux about the spray cone axis, [10].

$$-n.(-k\nabla T) = h_g.(T_w - T_{sat}) \quad (9)$$

The heat transfer coefficient h_g at the upper surface of the workpiece was considered by the equation, [10]:

$$h_g = \frac{q}{T_w - T_{sat}} \quad (10)$$

The convection coefficient h_a exposed to atmospheric air is given by equation, [11]:

$$h_a = 1.42.\left(\frac{T_w - T_a}{h}\right)^{0.25} \quad (11)$$

The surface exposed to radiation. Then, the radiation boundary condition can be expressed as, [12]:

$$-n.q = \varepsilon.\sigma(T_a^4 - T_w^4) \quad (12)$$

3. MATERIALS AND METHODS

Chemical composition of the alloy elements used in wt.% were: Fe 63.14, Cr 29.31, Mo 3.7, Ni 3.0 and S 0.82. The alloy was atomized with argon and deposited onto a stainless steel substrate, positioned 600 mm below the atomization nozzle. Atomization pressure was set at 1x10^5 Pa and superheating of the melt at about 1650 K. The alloy was melted down by induction heating, cast at 1650 K and so it was atomized. The specimens were extracted from the center of the deposits for microstructural analysis.

Microstructural characterization studies were conducted on the polished, etched as-cast and it was analyzed by a Shimadzu SSX-550 SEM-FEG microscopy, an Olympus BX-51 optical microscope (OM) with a QColor 3 digital camera for the image capture. As well, X-ray diffraction (XRD) analysis were recorded at a scan speed of 0.2˚min−1, using Rigaku mark equipment, model: Ultima IV, X-ray diffractometer and power 40/30 kW.

4. RESULTS OF THE NUMERICAL SIMULATION

4.1 Solidification Process Analysis

To following will be performed transient temperature field analysis. The result of

solidification procedure by numerical simulation of the workpiece in the spray-forming process is shown in Fig. 3, where the isotherms are shown at different time of solidification, in Fig. 3a shows the solidification process at 300 s, in Fig. 3b displays the result at 5000 s and in last, Fig. 3c at 10000 s.

During the solification procedure by the spray-forming process, the distribution of droplet mass flux is deposited on the subtract and then the growth process of the workpiece solidification is performed as a function of time, this type of process was not simulated. In this work it was considered, as if the workpiece has already formed, to this effect, the boundary conditions were applied, where, the non-linear heat transfer coefficient are functions, at the lower part, on the sides of the workpiece (Eqs 5, 8 and 12) and at the upper part the Gaussian distribution of droplet mass flux (Eqs 8-12) were applied. The initial temperature was 1650 K and the phase change from liquid to solid was 1609 K, in this case the latent heat is presented in the properties thermophysical considered [4,7].

According to observation of the simulation result, at all times the temperature at the top is higher than at the bottom of the workpiece to be solidified, this is consistent with the experimental part, because the hot droplets are arriving each time, this induces that the top to become warmer than other parts of the workpiece. It is also observed that the periphery of the workpiece gets colder due to contact with the environment and the interior gets warmer as time goes by and it can still be seen, the hottest zone moves to the top of the workpiece. Therefore, in this result we can observe various isotherms as a function of time (Fig. 3).

4.2 Study of Thermal Gradient

In order to complement this work and to clarify the phenomena that occur during solidification, the thermal gradient of the workpiece during solidification was studied and in Fig. 4 and the result of numerical simulation is visualized. At the initial instances of 300 s during solidification, the contours of the thermal gradient are shown, at the inferior part where it has a low temperature range, the thermal gradient is high, however, at the upper part of the workpiece the thermal gradient is relatively lower, on the other hand, at the sides the thermal gradient is high, although it is lower than at the inferior part, but at the central part which is hotter and the gradient is very low. E.g. for a temperature of 5000 K (Fig. 4b), the thermal gradient in general is much lower than for a temperature of 300 K, as it should be noted, at the inferior part of the workpiece the thermal gradient is high, as well as at the sides, but at the upper part it has dropped drastically in relation to the previous figure (Fig. 4a), while, the hottest zone moved upwards, similarly to Fig. 3b, in this region the gradient is much higher than Fig. 4a (at 300 K), moreover, in the more curved regions the gradient is significantly high, for instance, where there is a neck-like. Otherwise, for a solidification temperature at 10000 K, the behavior was similar to Fig. 4b, the hottest part it moved a little higher, though, both in the inferior part and in the lateral peripheries, the thermal gradient is much lower than in the hottest zone and the hottest part is last in solidifying as is well known. From this result we infer that the thermal gradient has a behavior inversely proportional to the temperature.

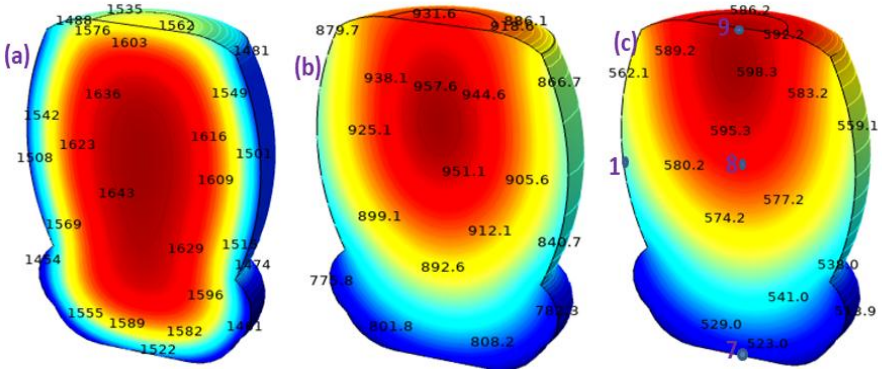

Fig. 3. Numerical simulation of workpiece solidified by spray-forming process. (a) at 300 s, (b) at 5000 s and (c) at 10000 s

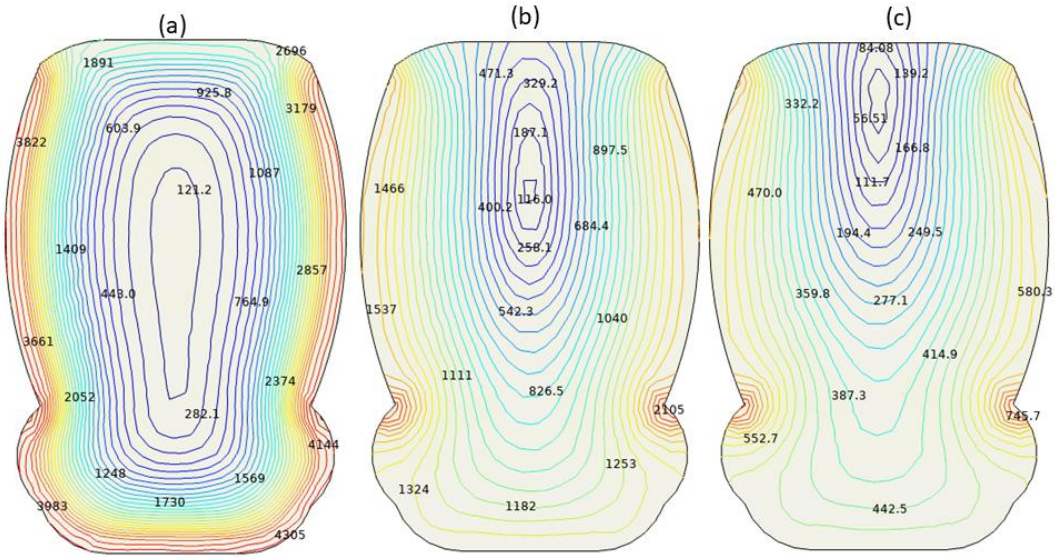

Fig. 4. Thermal gradient magnitude (k/m). (a) at 300 s, (b) at 5000 s and (c) at 10000 s

4.3 Cooling Curves Analysis

For study of cooling curves, different points were considered at the solidified workpiece (Fig. 3c), where the thermal gradient shows many changes, as shown in Fig. 4. The results of the cooling curves are shown in Fig. 5, e.g., in point 1, at the periphery and that corresponds to the workpiece belly, whose cooling curve (blue), in the first moments is high and soon after is relatively slow, is also observed the phase change (Fig. 5b) at around 20 s and the corresponding temperature is approximately 1610 K, that is consistent with Comsol [7] and Mi and Grant [4]. At point 7, which corresponds to the workpiece base, the cooling curve is high (green) and implies that the thermal gradient is high, in the first moments the thermal gradient is high, but as time goes the magnitude begins to decrease, as can be seen in Fig. 5, because this zone is the first to solidify that rest of the workpiece, whose phase change occurs at the same time as the previous case and the temperature corresponds is slightly higher than previous one. At point 9, the upper part of the workpiece, this region is warmer, consequently the solidification process is slower than previous cases, due to the recent hot droplets that arrive and also this one exposed to the environment, besides that, the phase change at this point occurs at the same instant as in previous cases, but the corresponding temperature is higher around 1630 K. Finally, point 8, during the solidification process, this region is warmer than the rest of the part, where the thermal gradient is low in the first moments, also when the solidification time increases and the thermal gradient increases, which can be verified in Fig. 5, in this region the solidification occurs last and the phase change is not appreciated in this figure, for this case, the phase change occurs around 300 s. This zone corresponds to the hottest zone in the first times and over time this hottest zone moves upwards (as in Fig. 3 or 4).

There are still few authors who work with the numerical simulation of solidification process by the Spray-Forming technique, between them, Zhang et al. [3] showed the result only in 2-D for IN718 Ni superalloy billet shapes in different times and other author, Cao et al. [12] who studied the formation mechanism of porosity for spray-deposited 7075 Alloy, however, they also simulated in 2-D the deposition predicting the porosity allied with the experimental result. It should be remarked, the form of the workship used (see Fig. 2a) in this work was similar to their experimental result [12].

4.4 Numerical Simulation and Experimental Correlation

In this work was made the numerical simulation of solidification by the Spray-forming process, using the thermophysical properties as a function of temperature for 21Cr-6Ni-9Mn alloy, supported by Comsol [7] and Mi and Grant [4]. The solidified piece in this work was similar to Fig. 2a. A microstructural and x-ray study of this alloy, processed by the spray-forming technique, was also carried out.

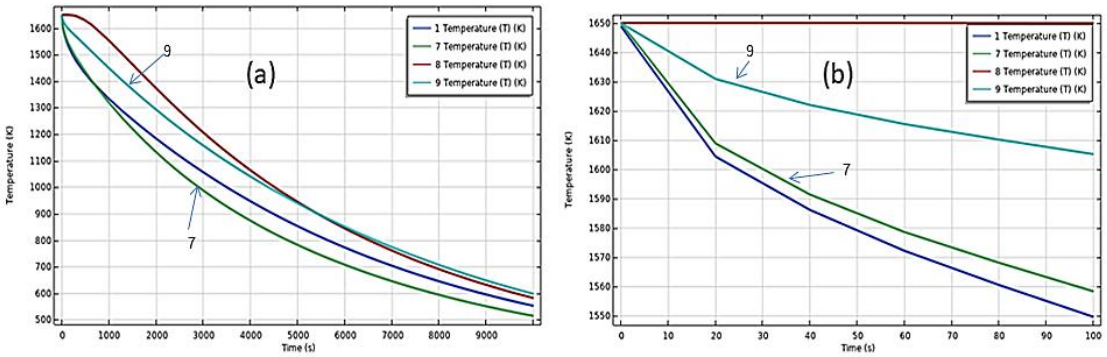

Fig. 5. Cooling curves at different points of the workpiece solidified by spray-forming process. (a) Cooling curves in total solidification time and (b) Cooling curves in the first moments of solification

According to the study by numerical simulation of the solidified workpiece (Fig. 6a), each point of this part can promote different microstructures that is related to the thermal history, for example, in the central zone of the workpiece has a microstructure presented in Fig. 6 b-c, where, Fig. 6b was performed with an optical microscope, however, in Fig. 6c presented was performed by SEM, it is to be pointed out, for this analysis, the solidified workpiece that found at room temperature, marking Fig. 6c, whose black needles are ferrite and the gray color between the needles is austenite. This result was confirmed by the different authors, among them, College [13], Wang et al. [14], Arun et al. [15] and Smuk [16], they reported that duplex stainless steel is the name given to the class of materials with biphasic microstructure, it is composed of a ferritic matrix and austenite islands, with volumetric fractions of approximately 50% of each phase.

Martins [17] confirmed that in the duplex and super duplex stainless steels obtained by casting process in sand molds, it is almost impossible to prevent sigma phase precipitation during solidification due to low cooling speed and this intermetallic significantly reduces the toughness and corrosion resistance of the material. However, by Spray Forming (SF) process, Zepon et al. [8], Kumar et al. [5] and Caoa et al. [12] found that a refined microstructure of the deposit, free of macro segregations, consisting of a uniform equiaxial structure of the matrix. Therefore, through this technique it is possible to avoid the sigma phase that originates in the traditional casting, such as using sand mold. In SF process the high solidification cooling rate is about 103 -105 K/s and in sand mold the solidification is low cooling speed.

Moreover, in this work the duplex stainless steel was investigated by X-ray diffraction analysis (XRD) that is shown Fig. 7, the standard XRD patterns of different metallic elements were identified, such as, Cr, Fe, Ni and meta-stable phases, among them, Fe-Cr, FeNi, Cr0.19Fe0.7Ni0.11, Ni-Cr-Fe and Cr1.36Fe0.52 and most of these phases are concentrated at the peak of greatest intensity, accompanied by the ferrite phase. The formation of these meta-stable phases is promoted by the high speed of cooling generated in the spray-forming process (Fig. 5), which leads also to the formation of the ferrite and austenite phases (Fig. 6c).

In super alloy processed by spray-forming, its microstructure characteristic depends of several factors, such as Mi and Grant et al. [4] investigated: (1) the geometrical and thermal conditions of the deposition surface, (2) the kinetic energy and thermal conditions of the impacting droplets, and (3) the interactions between the deposition surface and the impacting droplets. Moreover, also influence on this characteristic, the high cooling rate [103 -105 K/s] imposed by SF that enables achievement of refined microstructures with low segregation level, supersaturated solid solutions with metastable phases or even the formation of amorphous phases [8].

Duplex stainless steels are applied in various strategic areas, such as, supported by several authors, Sánchez-Tovar et al. [18] agreed upon that duplex stainless steels (DSSs) are balanced with two phases, ferrite and austenite. Therefore, DSSs are increasingly used because of their outstanding properties. For example, DSS high-mechanical strength, resulting from the balance of the duplex phases, allows its use in light-

weight components. Chai and Kangas [19] pointed out that new high alloyed duplex stainless steels with a combination of excellent corrosion resistance and higher high strength are needed. An important study by Li et al. [20] remarked, which duplex stainless steel (DSS) is widely used in various industries due to its desirable combination of excellent mechanical properties and corrosion resistance. Despite a very broad range of applications for DSS, there are still environments where the corrosion resistance of DSS is inadequate for long-term services. This means, more expensive materials with higher corrosion resistance are needed. Therefore, hyper duplex stainless steels (HDSSs) with a higher corrosion resistance are needed in some applications. This led to the development of highly alloyed HDSSs. Furthermore, Díaza et al. [21] pointed out that duplex stainless steels are finding increased application in the chemical, oil and gas industries, petrochemical process plants, the pulp and paper industry, pollution control equipment, transportation and for general engineering thanks to their outstanding corrosion resistance and mechanical properties.

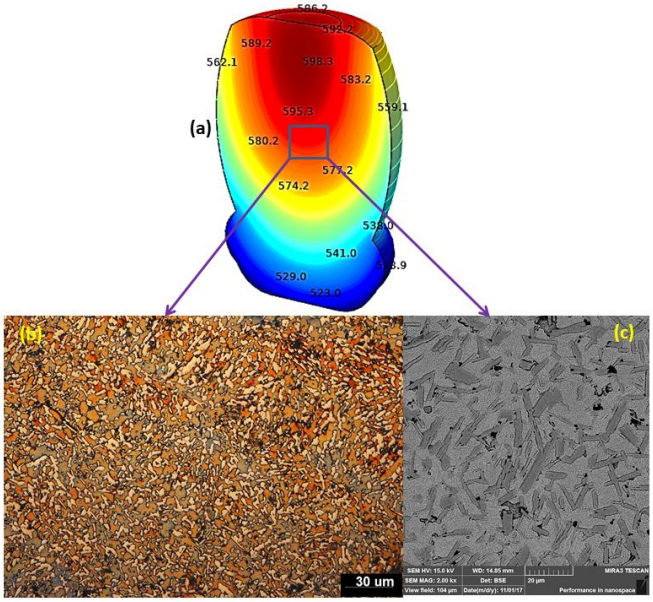

Fig. 6. Numerical simulation and experimental correlation (a) solidification at 10000 s, (b) optical and (c) SEM micrograph

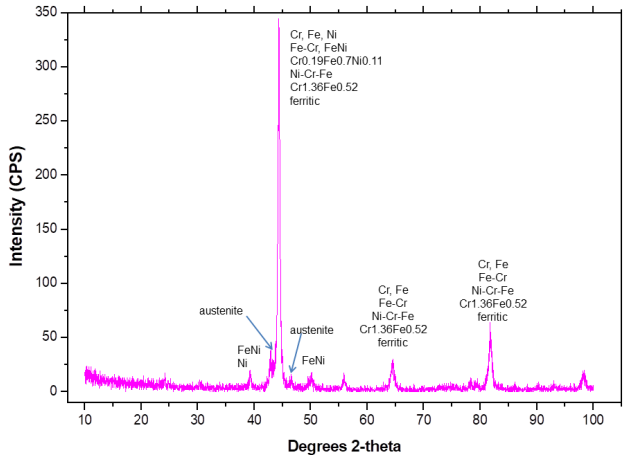

Fig. 7. XRD spectra of the duplex stainless steels

In addition to these studies, we also conducted the study of Vickers microhardness measurements in DSSs workpiece were carried out in this research. In this work the Vickers microhardness test was applied on workpiece of Fig. 6-b. As result, the microhardness Vickers (HV) was 460 with standard deviation of 14.7. Sousa et al. [22] reported that the material analyzed for super duplex stainless steel alloy exhibited a Vickers microhardness (HV) average value of 261 for austenite and 305 HV for ferrite, however, Bastos et al. [20] for same material presented a hardness value of 278 HV. Meanwhile, in this study Vickers microhardness measurements was around 460 HV, being much higher measured by the authors presented, this fact justifies, that this material was processed by Spray Forming (SF) technical, since, this technique promotes refined microstructures with low segregation level, supersaturated solid solutions with meta-stable phases or even the formation of amorphous phases. Consequently, rapid solidification simulated by the finite element technique of the duplex stainless steels leads to very high Vickers microhardness measurements, so the results are correlation and consistent.

Numerical simulation is a powerful tool to study many of critically important processes, as well as for the heat transfer conduction during solidification of droplet deposition. The challenging aspects in adoption of FEM in the spray-forming process sector is for to enable the application in manufacturing industry. The challenge in this work involved integrated of the thermophysical properties of material and application of boundary conditions, where non-linear heat transfer occurs and the solution process was performed in transient mode. For this purpose, a three-dimensional thermal transient finite element model has been developed to estimate the result.

Thus, in this work we found a good correlation of the numerical simulation result with the microstructural study, which were identified the ferrite and austenite phases, as well as the formation of metastable phases by the X-ray technique related to the high cooling speed (Fig. 5) during the spray-forming process. Therefore, through the result of numerical simulation we have a vision and a general forecast of the phenomena that occur during solidification, thus allowing us to control and get a good idea of the parameters that involve the experimental process, thereby saving time and cost of equipment.

4. CONCLUSION

In this research, heat transfer analysis using finite element modeling was carried out to study of solidification of droplet deposition in spray-forming process, applied boundary conditions non-linear of heat transfer coefficient in 3-D geometry. As result were the following.

1) In solidification process analysis, the isotherms are not uniform, they move according to the solification time, the hottest part that remains on the inside of the workpiece and it moves upwards as it cools,
2) The thermal gradient is very high at the beginning of solidification, with greater intensity in the zones that have high cooling, in the lower part of the workpiece and the contour lines of the thermal gradient move upwards following the hottest zone,
3) Faster cooling occurs at the bottom of the workpiece, and slow cooling occurs at the hot zone inside the workpiece.
4) Ferrite and austenite phases, as well as the formation of metastable phases by X-ray technique were identified, related to the high cooling speed during the spray-forming process,
5) A good correlation of the numerical simulation result with the microstructural study was found,
6) Duplex stainless steel is widely used in various industries due to its desirable combination of excellent mechanical properties and corrosion resistance.
7) Numerical simulation is a powerful tool to study the spray-forming process. The parameters that involve this process can save runtime experimental and cost of equipment, besides, predict the result.
8) The further research will be integrated melt atomization with droplet deposition process that involved transport phenomena.

ACKNOWLEDGEMENTS

This work was entirely financed by CNPq (Brazilian National Council for Scientific and Technological Development), FINEP (Research and Projects Financing Agency) and to LABMU–UEPG laboratory.

COMPETING INTERESTS

Authors have declared that no competing interests exist.

REFERENCES

1. Daha MA, Nassef GA, Abdallah IA, AbouSeeda HM. Three-dimensional thermal finite element modeling for keyhole plasma arc welding of 2205 duplex stainless steel plates. International Journal of Engineering and Technology. 2012;2:720-728.
2. del Coz Díaza JJ, Rodrígueza PM, Nietob PJG, Castro-Fresn D. Comparative analysis of TIG welding distortions between austenitic and duplex stainless steels by FEM. Applied Thermal Engineering. 2010;30:2448-2459. DOI: ORG/10.1016/J.APPLTHERMALENG.2010.06.016
3. Zhang G, Li Z, Zhang Y, Mi J, Grant PS. Modeling the deposition dynamics of a twin-atomizer spray forming system. Metallurgical and Materials Transactions B. 2010;41:303–307. DOI: 10.1007/s11663-009-9333-0
4. Mi J, Grant PS. Modelling the shape and thermal dynamics of Ni super alloy rings during spray forming Part 1: Shape modelling – Droplet deposition, splashing and redeposition. Acta Materialia, 2008;56(I):1588–1596. DOI: 10.1016/j.actamat.2007.12.021
5. Kumar S, Jadhav P, Patil A, Kirwai S, Singh R. An investigation of performance of spray formed H13 tool steel. Procedia Structural Integrity. 2019;14:872–882. DOI: 10.1016/j.prostr.2019.07.066
6. Mia J, Grant PS, Fritschingb U, Belkessamb O, Garmendiac I, Landaberea A. Multiphysics modelling of the spray forming process. Materials Science and Engineering A. 2008;477:2–8.
7. COMSOL Software, Stockholm, Sweden; 2017.
8. Zepon G, Ellendt N, Uhlenwinkel V, Bolfarini C. Solidification sequence of spray-formed steels. Metallurgical And Materials Transactions A. 2015;47:1-10. DOI: 10.1007/s11661-015-3253-1
9. Caoa F, Lia H, Ninga Z, Jiaa Y, Gua X, Yua L, Liua Z, Suna J. The formation mechanism of porosity for spray-deposited 7075 alloy. Materials Research. 2015;18:89-94. DOI: http://dx.doi.org/10.1590/1516-1439.328414
10. Mzad H, Khelif R. Effect of spraying pressure on spray cooling enhancement of beryllium-copper alloy plate. Procedia Engineering. 2016;157:106–113. DOI: 10.1016/j.proeng.2016.08.344
11. Tebbal M, Mzad H. An hydrodynamic study of a water jet dispersion beneathliquid sprayers. Forschung im Ingenieurwesen. Springer-Verlag. 2004;68:126–132. DOI: 10.1007/s10010-003-0118-3
12. Caoa F, Lia H, Ninga Z, Jiaa Y, Gua X, Yua L, Liua Z, Suna J. The formation mechanism of porosity for spray-deposited 7075 alloy. Materials Research. 2015;18:89-94.
13. College SS St. E. Microstructure of super-duplex stainless steels. Doctor of Philosophy at the University of Cambridge; 1993.
14. Wang S, Ma Q, Li Y. Characterization of microstructure, mechanical properties and corrosion resistance of dissimilar welded joint between 2205 duplex stainless steel and 16MnR. Materials and Design. 2011;32:831–837. DOI: 10.1016/j.matdes.2010.07.012
15. Arun D, Devendranath Ramkumar K, Vimala R. Multi-pass arc welding techniques of 12mm thick super-duplex stainless steel. Journal of Materials Processing Technology. 2019;271:126-143. DOI: 10.1016/j.jmatprotec.2019.03.031
16. Smuk O. Microstructure and properties of modern P/M super duplex stainless steels. Doctoral thesis, Dpto of Materials Science and Engineering, Royal Institute of Technology, Stockholm; 2004.
17. Martins M. Microstructural-mechanical characterization and corrosion resistance of super duplex stainless steel ASTM A890 / A890M Grade 6A, Doctoral Thesis (in Portugese), Universidade de São Paulo, Interunidades EESC-IFSC-IQSC; 2006.
18. Sánchez-Tovar R, Leiva-García R, García-Antón J. Characterization of thermal oxide films formed on a duplex stainless steel by means of confocal-Raman microscopy and electrochemical techniques. Thin Solid Films. 2015;576:1-10. DOI: ORG/10.1016/J.TSF.2014.12.024
19. Chai G, Kangas P. Super and hyper duplex stainless steels: structures, properties and applications. Procedia Structural Integrity. 2016;2:1755–1762. DOI: 10.1016/j.prostr.2016.06.221
20. Li H, Zhou E, Zhang D, Xu D, Xia J, Yang C, Feng H, Jiang Z, Li X, Gu T, Ke Yang.

Microbiologically influenced corrosion of 2707 hyper-duplex stainless steel by marine pseudomonas aeruginosa biofilm. Scientific Reports. 2016;6:1-12.
DOI: 10.1038/srep20190

21. del Coz Díaza JJ, Rodrígueza PM, Nietob PJG, Castro-Fresn D. Comparative analysis of TIG welding distortions between austenitic and duplex stainless steels by FEM. Applied Thermal Engineering. 2010;30:2448-2459.
DOI:ORG/10.1016/J.APPLTHERMALENG.2010.06.016

22. Souza EC, Rossitti SM, Rollo JMD. Influence of chloride ion concentration and temperature on the electrochemical properties of passive films formed on a superduplex stainless steel, Materials Characterization. 2010;61:240-244.
Available:https://doi.org/10.1016/j.matchar.2009.12.004

Peer-review history:
The peer review history for this paper can be accessed here:
http://www.sdiarticle4.com/review-history/69830